Available online at www.sciencedirect.com
SCIENCE DIRECT
Polymer 46 (2005) 7066–7071
polymer
www.elsevier.com/locate/polymer

Poly(vinyl alcohol)–poly(acrylic acid) interpenetrating networks. Study on phase separation and molecular motions

Rebeca Hernández, Ernesto Pérez, Carmen Mijangos, Daniel López*

Instituto de Ciencia y Tecnología de Polímeros, CSIC, c/Juan de la Cierva 3, Madrid 28006, Spain

Received 9 December 2004; received in revised form 6 April 2005; accepted 13 May 2005
Available online 17 June 2005

Abstract

We report on the preparation and characterization of interpenetrating polymer networks (IPNs) composed of poly(vinyl alcohol) (PVA) and poly(acrylic acid) (PAAc) formed by a sequential method. Interpolymer interactions were examined using ^{13}C CP/MAS NMR and DSC methods. Evidence on the formation of a PVA–PAAc complex through hydrogen bonds between the hydroxyl groups of the PVA chains and the carbonyl group of the PAAc chains was obtained. The existence of polymer interactions between PVA and PAAc and its effect on the molecular motion of polymer chains, was further investigated by means of the analysis of the ^{13}C spin–lattice relaxation times in the rotating frame, $T_{1\rho}^{C}$. To elucidate the scale of the mixing in the PVA/PAAc IPNs, proton spin–lattice relaxation times in the rotating frame, $T_{1\rho}^{H}$, were also investigated. The analysis of the results reveals the compatibility between the PVA and the PAAc polymer networks at low PVA concentrations and the occurrence of phase separation at relatively high PVA concentrations.

Keywords: Interpenetrating networks; Polymer interactions; Miscibility

1. Introduction

Interpenetrating polymer networks (IPNs) are a combination of two or more polymer networks synthesized in juxtaposition [1]. They can also be described as polymer networks held together by permanent entanglements. The networks are held by topological bonds, essentially without covalent bonds between them. By definition, an IPN structure is obtained when at least one polymer network is synthesized independently in the immediate presence of another. IPNs are an important class of materials attracting broad interest from both fundamental and application points of view [2,3].

The fundamental phenomenon associated with all IPN's is that phase separation occurs during the reaction. The timing and the extent of phase separation are determined by the thermodynamic immiscibility changes during the course of the reaction [4]. The extent of phase separation is limited by the spatial scale over which interpenetration occurs at the onset of phase separation, and this in turn is related to the rates of polymerization in the system.

Differential scanning calorimetry (DSC) has been mostly used to study polymer miscibility. The detection of a single glass transition temperature, T_g, is generally considered as evidence of compatibility [5]. The glass transition temperatures of miscible systems lay between the T_g values of the component polymers, and may go through a maximum as a function of concentration if strong specific interactions occur between polymers [6]. It is interesting to use this general approach to study the interpenetrating character of IPNs. Solid state NMR spectroscopy has an advantage over other techniques for studying multi component polymer systems: it can be used to determine not only the level of miscibility but also the motion of the individual homopolymers [7,8]. In the past, molecular motion in polymer blends has been studied by a number of techniques, e.g. DMA, dielectric spectroscopy and DSC. However, in principle these techniques allow only to study the bulk dynamic properties or the motion of only a single component of the blend. It is demonstrated that blends classified as miscible by the aforementioned methods may also display a pronounced heterogeneity of chain motion as determined by NMR spectroscopy [9].

* Corresponding author. Tel.: +34 91 562 29 00; fax: +34 91 564 48 53.
E-mail address: daniel@ictp.csic.es (D. López).

0032-3861/$ - see front matter © 2005 Elsevier Ltd. All rights reserved.
doi:10.1016/j.polymer.2005.05.108

The ^{13}C cross polarization and magic angle spinning (CP/MAS) NMR technique enables one to obtain information on the molecular structure of polymers. While analysis of chemical shifts proved valuable, a potentially even more potent use of solid-state NMR for polymers is the study of molecular motions. NMR relaxation behavior provides details on molecular motion of the polymer chains [10], where the motional frequency studied is determined by the choice of the experiment.

^{13}C spin–lattice relaxation times in the rotating frame ($T_{1\rho}^{C}$) can be used to analyze the motion of polymer chain segments and side chains. Interactions between polymers change the molecular motion and these changes are reflected in the relaxation times. One can take advantage of the large chemical shift dispersion of ^{13}C to resolve nuclei in different chemical environments and measure relaxation rates at each resolvable carbon because the low abundance of ^{13}C precludes averaging of relaxation rates by spin diffusion. $T_{1\rho}^{C}$ relaxation times have been extensively used to study the local dynamics in bulk polymers below T_g [11,12]. A significant example is that of polycarbonate for which $T_{1\rho}^{C}$ determinations show that there is a large distribution of motions with frequencies of a few tens of kilohertz [13]. $T_{1\rho}^{C}$ has been measured in liquid-crystalline poly(ester amides) [14] and blends of poly(vinyl phenol) with poly(methyl acrylate or methacrylate) [15], and a variable temperature study of $T_{1\rho}^{C}$ in aromatic polyamide networks and swollen gels has also appeared [16].

^{1}H spin–lattice relaxation times in the rotating frame ($T_{1\rho}^{H}$) are a very powerful tool for monitoring the phase separated domains in immiscible polymer blends [17,18]. In a homogeneous sample, all protons relax at about the same rate via spin diffusion. In a blend, when the phase separated domains are larger than 1–2 nm, different proton relaxation rates may be observed. On the opposite, if carbon resonances associated to each homopolymer component exhibit the same $T_{1\rho}^{H}$ value, then the efficiency of the spin diffusion during the few milliseconds of the spin–lattice relaxation in the rotating frame indicates that the material is homogeneous at the length scale of 1–2 nm [19]. This criterion can be readily applied to investigate the chain environments of each IPN component [20].

On the other side, PVA and PAAc can form IPNs through a sequential method. These PVA/PAAc IPNs shows drastic swelling changes by external pH and temperature according to the repulsion of ionic groups and association–dissociation of hydrogen bonds between the two polymers. The release of drugs incorporated into these IPNs exhibits pulsatile patterns in response to both pH and temperature. Also, the permeabilities of various solutes through the PVA/PAAc IPNs are regulated as a function of temperature, pH, ionic strength, solute size and ionic properties of the solutes. These characteristics make these systems very interesting as controlled drug delivery systems [21–23]. However, the interpenetrating character of the PVA/PAAc IPNs has not been determined yet.

In this work, the preparation and the miscibility and microphase structure of these IPNs have been investigated by measuring the ^{1}H spin–lattice relaxation times in the rotating frame ($T_{1\rho}^{H}$) as well as through the T_g determination. The effect of the existence of polymer interactions between PVA and PAAc on the molecular motion of the polymer chains will be determined by the interpretation of ^{13}C spin–lattice relaxation times in the rotating frame ($T_{1\rho}^{C}$).

2. Experimental section

2.1. Materials and reagents

Acrylic acid monomer (AAc) was purchased from Aldrich and was purified under vacuum distillation to eliminate hydroquinone inhibitor. *N*,*N*′-methylenbisacrylamide (*N*-BAAm) used as crosslinker and potassium persulfate used as thermal initiator were employed without further purification. Poly(vinyl alcohol), >99% hydrolyzed, with a weight average molecular weight of 94.000 g/mol and a tacticity of syndio = 17.2%, hetero = 54.1% and iso = 28.7%, from Aldrich, was used without further purification.

2.2. Preparation of PVA/PAAc IPNs

PVA/PAAc IPNs were prepared by a sequential method: PVA solutions (polymer concentrations ranging from 3 to 10% (g/mL)) were prepared in hermetic Pyrex tubes by mixing the appropriate amount of polymer and water (milli-Q grade) at 100 °C under conditions of vigorous stirring until the polymer was completely dissolved. Aqueous solutions of acrylic acid monomer, containing the thermal initiator and the crosslinking agent, were added at room temperature. The degree of crosslinking, *X*, is defined as the ratio of moles of crosslinking agent to moles of PAAc repeating units. The crosslinking degree thus achieved was 3%. The solutions were poured into glass plates, sealed with paraffin and allowed to react at 50 °C for 24 h. After this, the specimens were subjected to a freezing-thawing cycle: they were frozen to −32 °C for 15 h and then, allowed to thaw at room temperature for 5 h. In order to eliminate reactants, gels were immersed in deionized water (pure gels) and kept there until equilibrium is attained at room temperature. Films were obtained by simple drying of the 'swollen' hydrogels at room temperature. The composition of the IPNs is shown in Table 1.

2.3. DSC measurements

The glass transition temperature (T_g) value of various samples were measured with a Perkin–Elmer DSC7 under nitrogen purge gas using a heating rate of 20 °C/min. Indium was used as a standard for calibration. Each sample was subjected to several heating/cooling cycles to obtain

Table 1
Composition of samples

Sample[a]	mol PVA	mol_{PVA}/mol_{PAAc}	C_{PAAc} (mol/L)	C_{PVA} (mol/L)	% weight PVA
PVA3PAAc3	0.027	0.5/1	1.25	0.6	25
PVA5PAAc3	0.045	0.9/1	1.25	1.1	35
PVA7PAAc3	0.063	1.2/1	1.25	1.5	44
PVA10PAAc3	0.09	1.8/1	1.25	2.25	52

[a] For all the samples: degree of crosslinking of PAAc 3%.

reproducible T_g values. The T_g is taken from the midpoint of the transitions in the DSC curves.

2.4. Solid state ^{13}C NMR experiments

Solid state ^{13}C NMR experiments were carried out using a Bruker Advance spectrometer at 400 MHz. High resolution ^{13}C NMR was performed using magic-angle sample spinning (MAS) and high power spin decoupling. To enhance the signal to noise ratio, the cross-polarization (CP) technique was applied. Zirconia rotors were used at a spinning velocity of 4.0 kHz. The $\pi/2$ pulse was 5.3 and 3.5 μs for ^{13}C and ^{1}H, respectively. The contact time for CP was 1 ms. Four thousand scans were necessary to obtain an adequate signal to noise ratio. The chemical shifts of ^{13}C spectra are reported in ppm relative to TMS by taking the methine carbon of solid adamantane (29.5 ppm) as an external reference standard. $T^{C}_{1\rho}$ experiment were carried out applying a ^{13}C spin-locking pulse after the CP time. The decay of the ^{13}C magnetization in the spin-locking field was followed for spin-locking times of up to 10 ms. Selective $T^{H}_{1\rho}$ measurements were performed using a spin-lock pulse sequence with a delayed contact time. In these experiments, six variable ^{1}H spin-lock delays from 0.01 up to 4 ms were used prior to CP.

The $T_{1\rho}$ values were calculated from [24]:

$$M_{(t)} = M_{(0)}\exp\left(-\frac{t}{T_\rho}\right) \tag{1}$$

where t is the spin-lock time used in the experiment, and $M_{(0)}$ and $M_{(t)}$ are the peak intensities at zero time and at t, respectively.

3. Results and discussion

3.1. Differential scanning calorimetry

If monomer conversion can be driven to completion and the T_gs of the two components are well separated, one should in principle be able to use the shifts in T_g values found in the IPN to infer phase mixing among the components. One approach to infer the extent of mixing employs the Fox equation [25]. For our system, the Fox equation can be expressed as:

$$\frac{1}{T_g} = \frac{w'_{PVA}}{T_{gPVA}} + \frac{w'_{PAAc}}{T_{gPAAc}} \tag{2}$$

where w'_{PVA} and w'_{PAAc} are the weight fractions of PVA and PAAc, respectively.

Many multi component polymer systems have T_g values higher than those calculated from the weight content values of the T_g values of the component polymers [26]. The high T_g value has been ascribed to interactions between the component polymers which act as physical crosslinks, thus reducing segment mobility. As shown in Fig. 1(a), the T_g values of the PVA/PAAc IPNs are higher than the theoretical values predicted by the Fox equation, which indicates the presence of interactions between PVA and PAAc. However, the broadness of the transition (Fig. 1(b)) suggests that there is no molecular compatibility between the polymers.

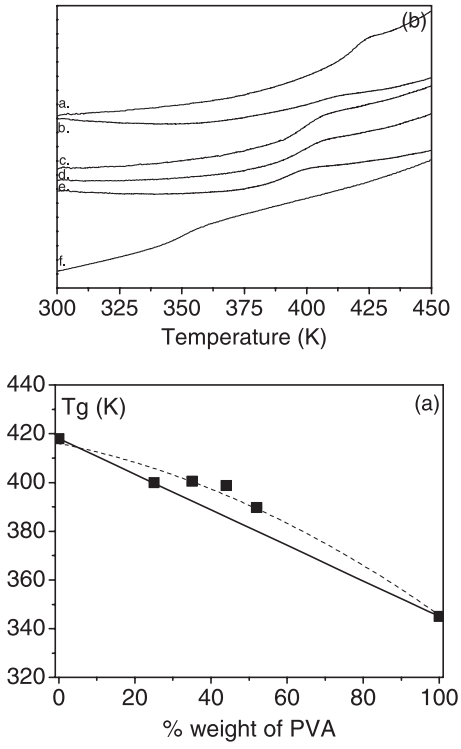

Fig. 1. (a) T_g-composition curve of PVA–PAAc IPNs. (■) experimental T_g values; (—) Fox equation and (b) DSC scans of samples: PAAc of crosslinking degree 3% (a); PVA (f) and PVA/PAAc3 IPNs of PVA concentrations: 3% (b); 5% (c); 7% (d) and 10% (e).

3.2. ^{13}C CP/MAS spectra and hydrogen bonding interaction

Evidence on interpolymer interactions in multicomponent polymer systems can be obtained from high-resolution solid state ^{13}C NMR as demonstrated by changes in chemical shift and/or line shape.

The ^{13}C CP/MAS spectra of PVA, PAAc and their interpenetrating networks are shown in Fig. 2. Assignments of ^{13}C spectra of PVA, PAAc were made by the reference to previous results reported in Ref. [27] and are shown in Table 2. Resonances of the COOH carbon of PAAc and CHOH carbon of PVA, whose chemical shifts are very sensitive to hydrogen bond formation, consist of well resolved peaks without any overlapping for all the samples. For pure PVA, the CHOH band shows three peaks in the solid state as previously reported [28]. Terao et al. [28] interpreted the chemical shifts of the CHOH resonance in terms of inter and intramolecular hydrogen bonding. They assigned peak 6 (Table 2) to the carbon which is linked by two hydrogen bonds to neighbor CHOH groups, peak 5 to the carbon linked by only one hydrogen bond, and peak 4 to the carbon not hydrogen bonded at all. Thus, peak 6 and 5 can be taken as indicators of inter- and intramolecular hydrogen bonding of OH groups between two units of the PVA chain (Table 2).

In the same way as for PVA/PAAc blends [29,30], a remarkable composition dependence of the ^{13}C NMR spectra was observed for PVA/PAAc IPNs. Peak 6 is not observed for any of the IPNs samples. This detail indicates that the formation of two hydrogen bonds over the same hydroxyl group is restricted. This can be interpreted by the formation of a PVA–PAAc complex through hydrogen bonds between the hydroxyl groups of the PVA chains and the carbonyl group of the PAAc chains. The steric hindrance introduced by the PAAc seems to inhibit the formation of more than one hydrogen bond per monomer unit.

Table 2
Peak assignment in the ^{13}C spectra of PAAc (crosslinking degree 3%) and PVA films

Peak	Assignment	δ (ppm)	
		PAAc 3%	PVA 10% (g/mL)
1	$-CH_2-$	34.1	
2	–CH–	40.9	
3	$-CH_2-$		45.8
4	–CH–		65.0
5	–CH–		70.6
6	–CH–		76.3
7	–CO(NH)–	177.7	
8	–COOH–	181.8	

The intermolecular interaction between PAAc and PVA chains is further confirmed by the upfield shift of peak 8. This detail can be observed in Fig. 3 which represents the region corresponding to the carbonyl peaks.

3.3. Relaxation time analysis

Further evidence of a blending effect on the motional state can be obtained from the $T_{1\rho}^{C}$ measurements because the low natural abundance of ^{13}C eliminates the effect of spin diffusion. Indeed, the $T_{1\rho}^{C}$ relaxation consists of two

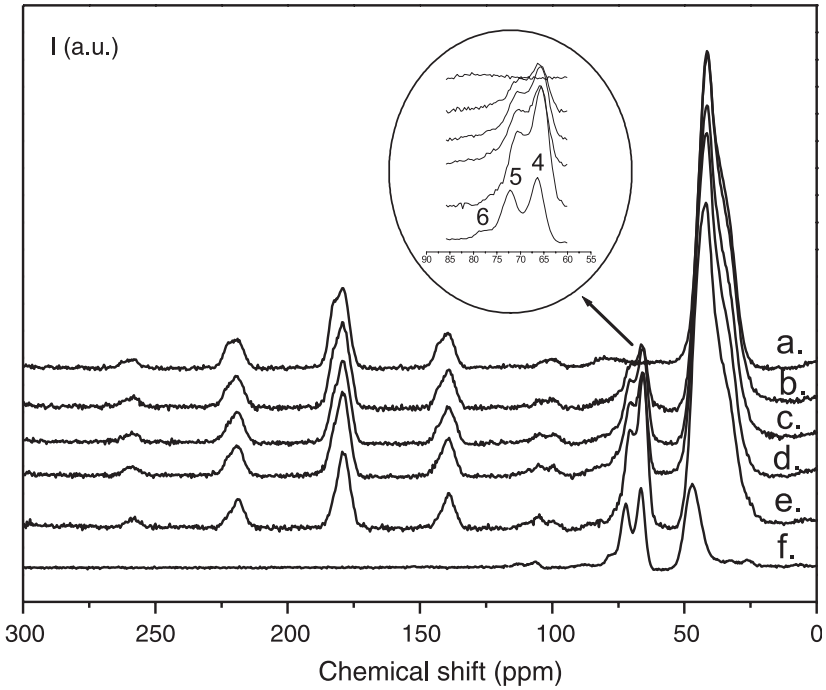

Fig. 2. ^{13}C CP/MAS spectra of dried films of: PVA (f), PAAc of crosslinking degree 3% (a) and PVA/PAAc3 IPNs of PVA concentrations 3% (b); 5% (c); 7% (d); and 10% (e).

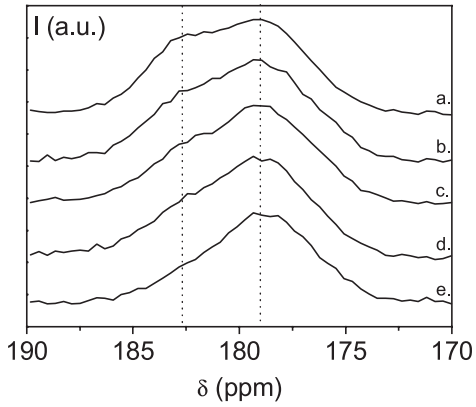

Fig. 3. ^{13}C CP/MAS spectra region corresponding to the carbonyl peaks. PAAc of crosslinking degree 3% (a) and PVA/PAAc3 IPNs of PVA concentration 3% (b); 5% (c); 7% (d); and 10% (e).

processes: spin–spin and spin–lattice relaxations. For highly crystalline rigid polymers, the strong static proton dipolar interaction makes the spin–spin process dominant in the relaxation. In such a case, however, the $T_{1\rho}^{C}$ provides no information about molecular dynamics [31]. On the other hand, for amorphous glassy polymer systems (which is the case of the systems presented in this paper) with internal local mobility the fluctuating dipolar fields are caused largely by the rotation of the ^{13}C–^{1}H internuclear vectors; the spin–lattice process is dominant [11]. $T_{1\rho}^{C}$ is sensitive to the motion of polymer chains in a frequency range of 10–100 kHz which occurs below the glass transition temperature. Fig. 4 shows the $T_{1\rho}^{C}$ decay curve as a function of spin locking time for different carbons in sample PVA5PAAc3 (PVA = 5% g/mL, crosslinking degree PAAc = 3%) at 298 K.

As in most glassy polymers the ^{13}C decay as a function of the spin locking time is not a single exponential. The nonlinearity in $T_{1\rho}^{C}$ plots can be interpreted to be due to the presence of a multiplicity of relaxation times for otherwise sharp (under magic angle spinning conditions) and well defined lines. This is the sort of phenomenon which might

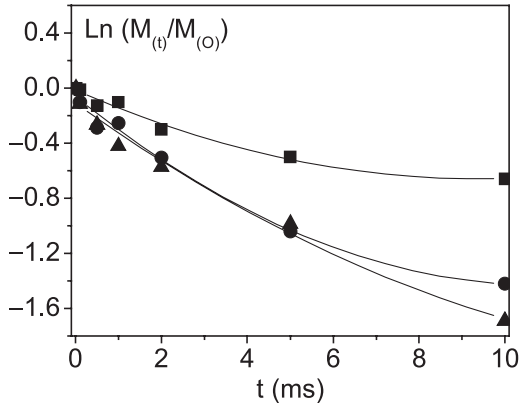

Fig. 4. $T_{1\rho}^{C}$ decay curve as a function of spin locking time for carbon 7, 8 (carbonyl region) (■); carbon 4 (●); carbon 5 (▲) for the sample PVA5PAAc3 (PVA = 5% g/mL, crosslinking degree PAAc = 3%).

be expected for mixed phase systems, in which the various component phases had significantly different motional properties described by significantly different relaxation times. An average $T_{1\rho}^{C}$ determined from the initial part of the curve has been thought to represent a large fraction of motions at frequencies in the kilohertz range [32]. Fig. 5 presents the variation of $T_{1\rho}^{C}$ as a function of PVA concentration. As can be observed, the resonances of PVA in the IPNs retain the same relaxation characteristics as in pure PVA. However, the $T_{1\rho}^{C}$ which corresponds to the carbonyl group resonance becomes longer with the introduction of PVA in the sample PVA3PAAc3 while for the other samples with higher PVA concentration, $T_{1\rho}^{C}$ remains constant with PVA concentration. That means that blending with PVA alters the motional state of PAAc. Therefore, only the environment of the hydrogen bond seems to be affected and there could be some PVA domains in these samples. It has been reported that in immiscible blends there is no observable change in $T_{1\rho}^{C}$ with blending [33].

To elucidate the scale of mixing in the PVA/PAAc IPNs, proton spin–lattice relaxation times in the rotating frame ($T_{1\rho}^{H}$) were determined and the values are represented in Fig. 6 as a function of PVA concentration. As can be observed, in the samples with PVA compositions of 25 and 35 wt%, as a result of spin diffusion, all carbons exhibit a single $T_{1\rho}^{H}$. For higher concentrations of PVA, PAAc carbons and PVA carbons exhibit different $T_{1\rho}^{H}$ which indicates that there is a higher degree of phase separation for these samples. These results are in agreement with previous results obtained in our group for PVA/PAAc IPNs [34]. The storage modulus of PVA/PAAc IPNs, as determined by viscoelastic measurements, increases with PVA concentration until a PVA concentration of around 30 wt% for the samples with a degree of crosslinking of PAAc of 6%. Above this PVA concentration the storage modulus decreases for all samples. This is probably due to the occurrence of a phase separation process, which results in an inhomogeneity of the samples and the loss of the

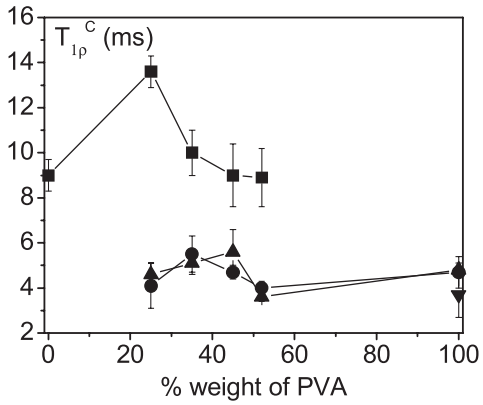

Fig. 5. $T_{1\rho}^{C}$ vs % weight of PVA: carbons 7, 8 (carbonyl region) (■); carbon 4 (●); carbon 5 (▲) and carbon 6 (▼).

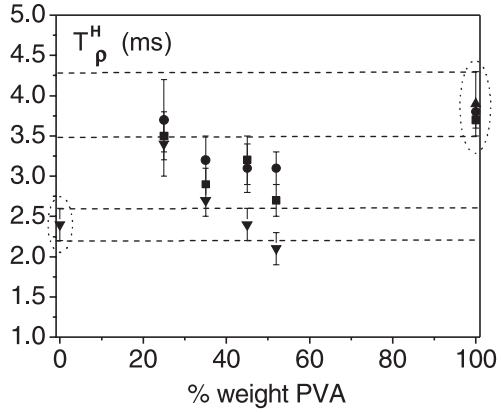

Fig. 6. $T^H_{1\rho}$ vs % weight of PVA: carbons 7, 8 (carbonyl region) (▼); carbon 4 (■); carbon 5 (●) and carbon 6 (▲).

mechanical properties. The inhomogeneity of the samples has also been shown by ATR spectroscopy [34].

4. Conclusions

We report a sequential method of preparation of PVA/PAAc interpenetrating polymer networks. The results obtained by DSC and ^{13}C CP/MAS NMR analysis of the samples point to the formation of a polymer–polymer complex through hydrogen bonds between the hydroxyl groups of PVA chains and the carbonyl groups of PAAc chains in the IPNs, hence confirming its interpenetrating character.

For all the IPNs prepared, the peaks in the ^{13}C CP/MAS spectra do not exhibit a single exponential $T^C_{1\rho}$ decay behavior. This fact can be interpreted to be due to the presence of a multiplicity of relaxation times. Such a result is in agreement with DSC measurements. The broadening of T_g arises from different space areas having different compositions, each one yielding its own T_g.

Samples with PVA compositions up to 25–30% show a single $T^H_{1\rho}$ value for all the carbons due to an efficient spin diffusion process. Above this concentration there exist different $T^H_{1\rho}$ values for carbons corresponding to PVA and to PAAc. This can be attributed to the segregation of PVA from the PAAc network due to phase separation.

Acknowledgements

The authors are grateful to the Spanish Ministerio de Educación y Ciencia (MEC) (MAT2002-0620) for financial support.

References

[1] Sperling LH. Interpenetrating polymer networks and related materials. New York: Plenum Press; 1981.
[2] Bischoff R, Cray SE. Prog Polym Sci 1999;24:185.
[3] Yahya R, Ahmad Y, Mitchell AW. Macromolecules 1999;32:3241.
[4] Mishra V, Sperling LH. Polymer 1995;36:3593.
[5] Olabisi O, Robeson LM, Shaw MT. Polymer–polymer miscibility. New York: Academic Press; 1979. p. 117–281.
[6] Natansohn A, Simmons A. Macromolecules 1989;22:1611.
[7] Schmidt-Rohr K, Clauss J, Spiess HW. Macromolecules 1992;25:3273.
[8] Chu CW, Dickinson LC, Chien JC. J Appl Polym Sci 1990;41:2311.
[9] Jack KS, Whittaker AK. Macromolecules 1997;30:3560.
[10] Bovey FA, Jelinsky LW. J Phys Chem 1985;89:571.
[11] Schaefer MD, Sefcik RA, McKay RA. Macromolecules 1981;14:188.
[12] Tekely P, Laupretre F, Monnerie L. Polymer 1985;26:108.
[13] Schaefer J, Sefcik MD, Stejskal EO, Steger TR, McKay RA, Dixon WT, et al. Macromolecules 1984;17:1107.
[14] Hatfield G, Aharoni SM. Macromolecules 1989;22:3807.
[15] Zhang X, Takegoshi K, Hikichi K. Macromolecules 1991;24:5756.
[16] Curran SA, Laclair CD, Aharoni SM. Macromolecules 1991;24:5903.
[17] McBrierty VJ, Douglass DC, Kwei TK. Macromolecules 1978;11:1265.
[18] Albent B, Jerome R, Teyssie P, Smyth G, Boyle NG, McBrierty VJ. Macromolecules 1985;18:388.
[19] VanderHart DL, Mc Fadden GB. Solid State Nucl Magn 1996;7:45.
[20] Brachais L, Laupretre F, Caille JR, Teyssié D, Boileau S. Polymer 2002;43:1829.
[21] Lee YM, Kim SH, Cho CS. J Appl Polym Sci 1998;69:479.
[22] Kim SY, Lee YM. J Appl Polym Sci 1999;74:1752.
[23] Kim SY, Shin HS, Lee YM. J Appl Polym 1999;73:1675.
[24] Bovey FA, Mirau PA. NMR of polymers. San Diego: Academic Press; 1996.
[25] Fox TG. Bull Am Phys Soc 1956;1:123.
[26] Yang J, Winnick MA, Ylitalo D, DeVoe RJ. Macromolecules 1996;29:7047.
[27] Neppel A, Eaton DR, Hunkeler D, Hamielec AE. Polymer 1988;29:1338.
[28] Terao T, Maeda S, Saika A. Macromolecules 1983;16:1535.
[29] Zhang X, Takegoshi K, Hikichi K. Polym J 1991;23:87.
[30] Zhang X, Takegoshi K, Hikichi K. Polymer 1992;33:712.
[31] VanderHart DL, Garroway AN. J Chem Phys 1979;41:2773.
[32] Schaefer J, Stejskal EO, Buchdahl R. Macromolecules 1977;10:384.
[33] Zhang X, Takegoshi K, Hikichi K. Macromolecules 1991;24:5756.
[34] Hernández R, Mijangos C, López D. J Polym Sci Part B Phys Ed. Submitted.